

Overproduction of thrombopoietin by *BRAFV600E*-mutated mouse hepatocytes and contribution of thrombopoietin to hepatocarcinogenesis

Hiroki Tanaka¹ | Kie Horioka¹ | Masahiro Yamamoto² | Masaru Asari¹ |
Katsuhiko Okuda¹ | Kosuke Yamazaki³ | Keiko Shimizu¹ | Katsuhiko Ogawa⁴ 

¹Department of Legal Medicine, Asahikawa Medical University, Asahikawa, Japan

²Department of Molecular Cancer Science, School of Medicine, Yamagata University, Yamagata, Japan

³Department of Clinical Medicine, Surgery Area, Japanese Red Cross Hokkaido College of Nursing, Kitamai, Japan

⁴Department of Pathology, Asahikawa Medical University, Asahikawa, Japan

Correspondence

Katsuhiko Ogawa, Department of Pathology, Asahikawa Medical University, Midorigaoka Higashi 2-1-1-1, Asahikawa Japan.
Email: ogawak@asahikawa-med.ac.jp

Funding information

Japanese Ministry of Education, Culture, Sports, Science and Technology, Grant/Award Number: JP16K14615

Abstract

In hepatocarcinogenesis induced by diethylnitrosamine (DEN) in B6C3F1 mice, the *BrafV637E* mutation, corresponding to the human *BRAFV600E* mutation, plays a pivotal role. The livers of transgenic mice with a hepatocyte-specific human *BRAFV600E* mutation weighed 4.5 times more than that of normal mice and consisted entirely of hepatocytes, resembling DEN-induced preneoplastic hepatocytes. However, these transgenic mice spontaneously died 7 wk after birth, therefore this study aimed to clarify the causes of death. In the transgenic mice, the liver showed thrombopoietin (TPO) overexpression, which is associated with eventual megakaryocytosis and thrombocytosis, and activated platelets were deposited in hepatic sinusoids. TPO was also overexpressed in the DEN-induced hepatic tumors, and sinusoidal platelet deposition was observed in the hepatic tumors of humans and mice. Podoplanin was expressed in some of the Kupffer cells in the liver of the transgenic mice, indicating that platelet activation occurred via the interaction of podoplanin with C-type lectin receptor 2 (CLEC-2) on the platelet membrane. Additionally, erythrocyte dyscrasia and glomerulonephropathy/interstitial pneumonia associated with platelet deposition were observed. In the transgenic mice, aspirin (Asp) administration prevented platelet activation, reduced the liver/body weight ratio, decreased the platelet deposition in the liver, kidney, and lung, and prevented erythrocyte dyscrasia and ameliorated the renal/pulmonary changes. Thrombopoietin overproduction by *BRAFV600E*-mutated hepatocytes may contribute to hepatocyte proliferation via thrombocytosis, platelet activation, and the interaction of platelets with hepatic sinusoidal cells, while hematologic, renal, and pulmonary disorders due to aberrant platelet activation may lead to spontaneous death in the transgenic mice.

KEYWORDS

hepatic sinusoidal cells, hepatocarcinogenesis, platelets, preneoplastic hepatocytes, thrombopoietin

Abbreviations: Alb-Cre, Albumin-Cre-recombinase; Asp, aspirin; B6, C57BL/6; CLEC-2, C-type lectin receptor 2; DEN, diethylnitrosamine; HCC, hepatocellular carcinoma; LSEC, liver sinusoidal endothelial cells; PF4, platelet factor 4; TPO, thrombopoietin.

This is an open access article under the terms of the Creative Commons Attribution-NonCommercial License, which permits use, distribution and reproduction in any medium, provided the original work is properly cited and is not used for commercial purposes.

© 2019 The Authors. *Cancer Science* published by John Wiley & Sons Australia, Ltd on behalf of Japanese Cancer Association.

1 | INTRODUCTION

Hepatocarcinogenesis starts with the generation of carcinogenically altered hepatocytes. Following liver damage caused by chronic viral hepatitis, metabolic steatosis, or alcohol-induced injury, carcinogenically altered hepatocytes are forced to expand by the cytokine, chemokine, and growth factor milieu derived from chronic hepatic injury, inflammation, and restorative proliferation, resulting in the formation of preneoplastic nodules from which early hepatocellular carcinomas (HCCs) initiate, eventually leading to progressed and advanced HCC.¹

The mouse model of hepatic tumor induced by neonatal treatment with diethylnitrosamine (DEN) has been often used for investigation of hepatocarcinogenesis.² In this model, carcinogenically altered preneoplastic hepatocytes emerged at the earliest stage and eventually progressed into preneoplastic foci, adenomas, and HCC.³ The carcinogenic process is driven by either an *H-ras* or a *Braf* mutation.⁴⁻⁶ The role of the mutation is dependent on the animal's genetic background: in hepatocarcinogenesis-sensitive C3H mice, the *H-ras* codon 61 mutation is prevalent, while in hepatocarcinogenesis-resistant C57BL/6 (B6) mice, the *BrafV637E* mutation is preferentially selected.⁷

We have previously reported that *Albumin-Cre-recombinase* (*Alb-Cre*)/*BRAFV600E* transgenic mice that express the human *BRAFV600E* mutation, corresponding to the mouse *BrafV637E* mutation, specifically in hepatocytes from the B6 mouse genetic background showed a marked increase in liver size (four- to five-fold larger liver/body weight ratio than normal mice), and the liver consisted entirely of hepatocytes that resembled DEN-induced preneoplastic hepatocytes.⁸ This model therefore enabled us to investigate biological events that occurred within the early preneoplastic lesions induced by neonatal treatment with DEN. However, although these mice were healthy at birth, they spontaneously died at 7 wk of age due to unknown reason(s).

In this study, we aimed to clarify the cause of death in the *BRAFV600E* transgenic mice by analyzing the blood and tissue specimens isolated from the transgenic mice. Our current findings showed that the hepatocytes in *Alb-Cre/BRAFV600E* transgenic mice overproduced thrombopoietin (TPO), and this overproduction eventually resulted in megakaryocytosis and thrombocytosis; platelets were activated in the peripheral blood; and large numbers of platelets were deposited in liver sinusoids. Furthermore, podoplanin, which can activate platelets via C-type lectin receptor 2 (CLEC-2) on the platelet membrane,⁹⁻¹¹ was expressed in some of the Kupffer cells in the liver of *Alb-Cre/BRAFV600E* transgenic mice. Additionally, these mice showed erythrocyte dyscrasia, glomerulonephropathy, and interstitial pneumonia, which were thought to be derived from the deposition of aberrantly activated platelets. Our data suggested that the TPO-mediated macroenvironmental changes involving the liver and bone marrow may promote proliferation of the *BRAFV600E*-mutated hepatocytes, but cause hematological, renal, and pulmonary disorders that lead to death.

2 | MATERIALS AND METHODS

2.1 | Experimental animals

Male *Alb-Cre/BRAFV600E* transgenic (5–13 wk of age), and age-matched control *BRAFV600E* and C57BL/6 mice (Charles River Japan) were used in this study. *Alb-Cre/BRAFV600E* transgenic and control *BRAFV600E* mice were generated by in vitro fertilization using homozygous male *BRAFV600E* mice [B6.129P2(Cg)-*Bra*tm1Mmcm>/J; Jackson] and heterozygous female *Alb-Cre* mice (Jackson) as described previously.⁸ The male litters were genotyped to separate the *Alb-Cre/BRAFV600E* transgenic and control *BRAFV600E* mice with and without the *Alb-Cre* gene. Some of the *Alb-Cre/BRAFV600E* transgenic and control *BRAFV600E* mice were given aspirin (Asp) at a daily dose of 5 µg/g body weight by oral intubation from 4 to 8 wk after birth. Hepatic tumors were induced by neonatal treatment with 5 µg/g body weight of DEN on day 15 after birth in male B6C3F1 mice (Charles River Japan), and the tumor samples were collected at 8–12 mo of age. The mice were housed in plastic cages with sterilized wood chips and given a standard chow diet (CMF, Oriental Yeast) and sterilized water ad libitum. The mouse breeding room was kept at 25°C with a 12 h light and 12 h dark cycle. All procedures performed on mice were approved by the Asahikawa Medical University Animal Experiment Committee following the guidelines for the humane care and protection of animals.

2.2 | Human materials

Paraffin-embedded human hepatic tumor materials taken from patients who received hepatic biopsy or hepatectomy surgery during 2015–2018 in the affiliated hospital of Asahikawa Medical University were collected. All patients gave informed consent, and the study was approved by the ethical committee at the hospital.

2.3 | Antibodies

The antibodies used were against CD31 (Novus), CD61 (Cell Signaling), F4/80 (R&D Systems), podoplanin (R&D Systems), TPO (LSBio), Stat3 (Cell Signaling), S727 phospho-Stat3 (Cell Signaling), Y705 phospho-Stat3 (Cell Signaling) and α -tubulin (Novus).

2.4 | Hematological analysis

Complete blood count analyses were performed using an automated hematology analyzer (Sysmex). Peripheral blood and bone marrow smear samples were processed for May-Giemsa staining and examined under a microscope.

2.5 | Hepatocyte culture

Hepatocytes were isolated by collagenase perfusion from *Alb-Cre/BRAFV600E* and normal B6 mice at the age of 8 wk, purified by low speed centrifugation and cultured in Williams' E medium

supplemented with 10% fetal bovine serum and antibiotics for 12 h, followed by incubation with serum-free Williams' E medium for 24 h to collect the conditioned medium.

2.6 | Enzyme-linked immunosorbent assay

Platelet factor 4 (PF4) and TPO levels were analyzed using enzyme-linked immunosorbent assay kits (R&D Systems) according to the manufacturer's instructions.

2.7 | Real-time quantitative reverse transcription (qRT)-polymerase chain reaction (PCR)

RNA was extracted from liver tissue using an RNeasy Mini Kit (Qiagen). cDNA was reverse-transcribed from RNA using a high-capacity cDNA reverse transcription kit (Thermo Fisher). The expression levels of mouse TPO mRNA were then analyzed using a real-time PCR system (Thermo Fisher) with the TaqMan probe for mouse TPO mRNA (Thermo Fisher). mRNA expression was normalized to 18S rRNA expression.

2.8 | Western blotting

Tissue samples were lysed in RIPA buffer, separated by polyacrylamide gel electrophoresis and electrotransferred to nitrocellulose membranes. The membranes were probed with the primary antibodies and then incubated with a horseradish peroxidase (HRP)-conjugated anti-mouse or anti-rabbit IgG secondary antibody (R&D Systems). Antibody binding was visualized using the SuperSignal West Pico chemiluminescent substrate (Thermo Fisher).

2.9 | Histopathology, immunohistochemistry, and immunofluorescence

Tissues were fixed in 10% formalin in phosphate-buffered saline (PBS), paraffin-embedded and stained with hematoxylin and eosin (H&E). For live mice, the liver was perfused with PBS via the portal vein at 2-3 mL/min under ether anesthesia, followed by perfusion-fixation with 10% formalin in PBS. For immunohistochemistry, after deparaffinization, rehydration, and antigen retrieval, the tissue sections were incubated with the primary antibodies, followed by incubation with an HRP-conjugated anti-mouse or anti-rabbit IgG secondary antibody (Vector). For immunofluorescence, after quenching autofluorescence with the MaxBlock™ Autofluorescence Reducing Kit (Maxvision), the tissue sections were incubated with the primary antibodies and then with an Alexa Fluor (598/488)-conjugated anti-mouse or rabbit IgG secondary antibody (Thermo Fisher). Fluorescence images were analyzed using a fluorescence microscope (BZ-X700, Keyence).

2.10 | Electron microscopy

Renal tissues were fixed with a cacodylate-buffered glutaraldehyde solution followed by osmic acid fixation, dehydration, epoxy resin

embedding, and ultrathin sectioning. The sections were examined using an electron microscope (JEOL).

2.11 | Statistics

The differences in the experimental values of *Alb-Cre/BRAFV600E* transgenic mice and those of control *BRAFV600E* or normal B6 mice were statistically analyzed using Student's paired *t* test or the chi-squared test.

3 | RESULTS

3.1 | Spontaneous death and hematological changes in the *Alb-Cre/BRAFV600E* transgenic mice

Although the *Alb-Cre/BRAFV600E* transgenic mice were healthy at birth, 8 of 18 (44.4%) mice spontaneously died between 7 and 13 wk after birth (Figure 1). To clarify the cause of death, we not only performed autopsies on the dead mice but also sacrificed the live mice to collect blood and tissue samples between 5 and 13 wk after birth. The complete blood count analysis for the live mice 8 wk after birth revealed that platelet counts were significantly increased in *Alb-Cre/BRAFV600E* transgenic mice compared with the control *BRAFV600E* mice (Figure 2A) or normal B6 mice (data not shown). There were no significant differences in the white blood cell and red blood cell counts and the hemoglobin and hematocrit levels between the *Alb-Cre/BRAFV600E* transgenic and control *BRAFV600E* mice (data not shown). Consistent with thrombocytosis in the peripheral blood, the number of megakaryocytes was increased 10-fold in the bone marrow smear samples and tissue sections of the bone marrow and spleen in the *Alb-Cre/BRAFV600E* transgenic mice compared with the control *BRAFV600E* mice (Figure 2B-H). A few mitotic megakaryocytes were observed in the bone marrow of the *Alb-Cre/BRAFV600E* transgenic mice, but not in the control or normal mice (Figure 2F inset). We also

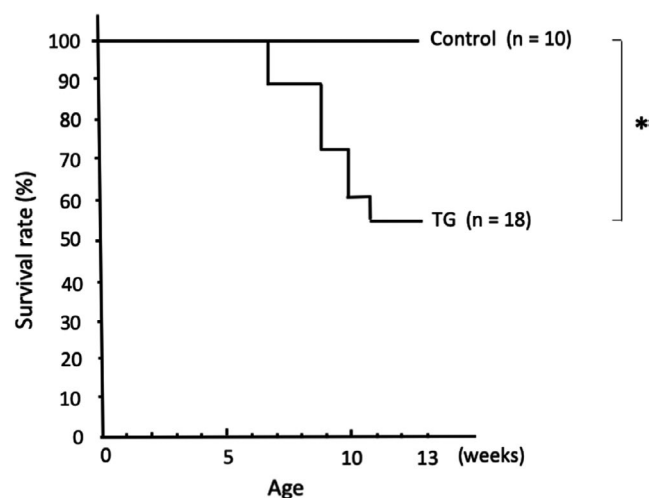


FIGURE 1 A Kaplan-Meier plot of the survival rate in control *BRAFV600E* mice (control) and *Alb-Cre/BRAFV600E* transgenic mice (TG) until 13 wk after birth; **P* < .01

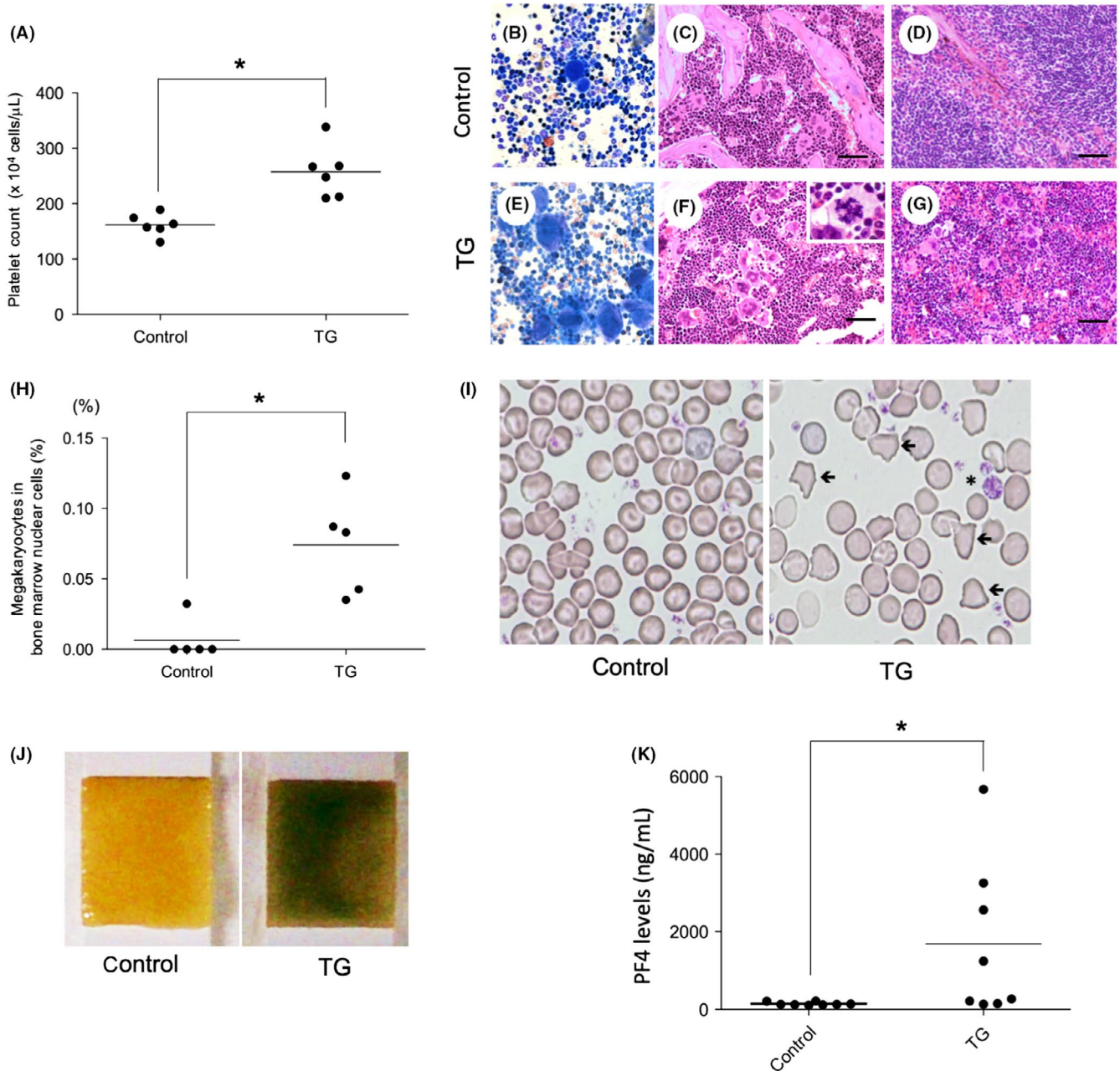


FIGURE 2 Hematological changes in *Alb-Cre/BRAFV600E* transgenic mice. A–K, control; 8-wk-old control *BRAFV600E* mice, TG; 8-wk-old *Alb-Cre/BRAFV600E* transgenic mice. A, Increased numbers of platelets in TG. * $P < .05$. B–G, Increase in the numbers of megakaryocytes in TG, (B, E) bone marrow smears, (C, F) bone marrow and (D, G) spleen tissues. Inset in F: mitotic display of a megakaryocyte. B, E, May-Giemsa staining; C, D, F, G, H&E staining; scale bars: 200 μ m. H, Increased numbers of megakaryocytes in bone marrow in TG; * $P < .01$. I, Peripheral blood smear. Schizocytes (arrows) and an enlarged platelet (*) in TG. J, Positive urinary hemoglobin test in TG. K, Increased platelet factor 4 (PF4) levels in TG; * $P < .05$

observed schizocytes (fragmented or abnormally shaped red blood cells) and enlarged platelets in the peripheral blood smears of the *Alb-Cre/BRAFV600E* transgenic mice (Figure 2I). Urine analyses revealed a positive reaction for hemoglobin, presumably due to hemoglobinuria caused by red blood cell destruction as well as hematuria derived from glomerulonephropathy as described below (Figure 2J). Because schizocytes are generated in association with thrombotic microangiopathy characterized by aberrant platelet activation and formation of fibrin mesh within blood,¹² we investigated the plasma levels of PF4, which

is released from α -granules in association with platelet activation.¹³ The PF4 levels were elevated in most *Alb-Cre/BRAFV600E* transgenic mice (Figure 2K).

3.2 | TPO overproduction in the liver of *Alb-Cre/BRAFV600E* transgenic mice

Thrombopoietin stimulates the differentiation of megakaryocytes from hematopoietic stem cells and the generation of platelets

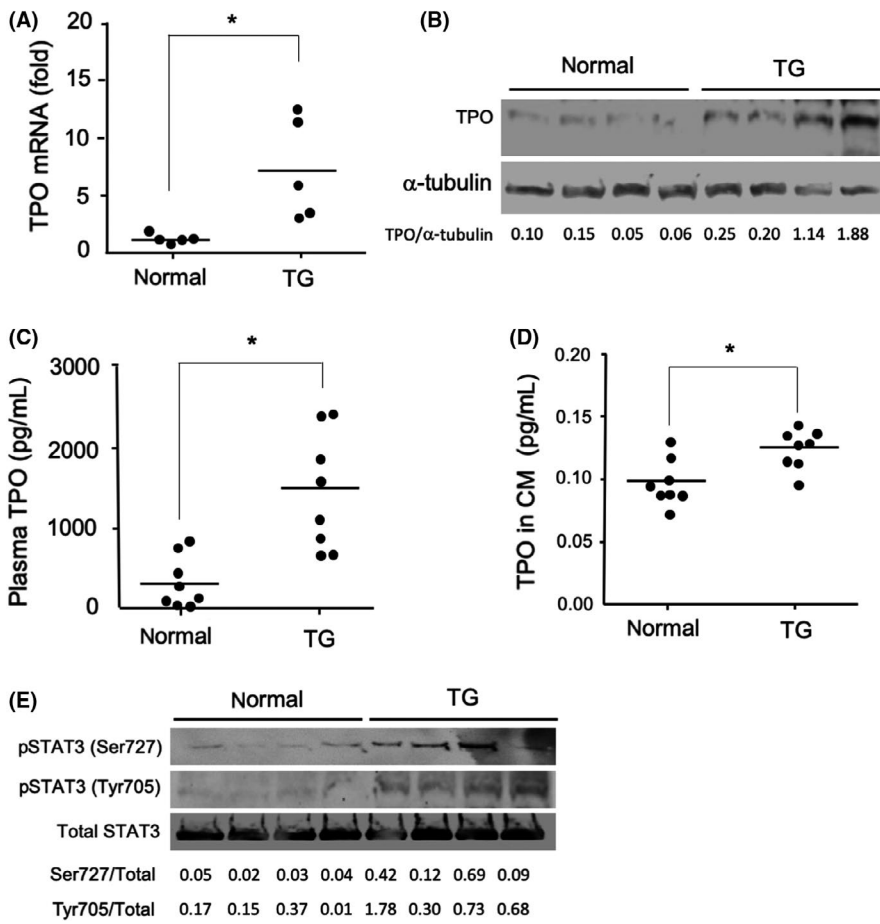


FIGURE 3 Thrombopoietin (TPO) overproduction and Stat3 activation in the liver of *Alb-Cre/BRAFV600E* transgenic mice. A–E, normal; normal B6 mice, TG; *Alb-Cre/BRAFV600E* transgenic mice. A, Increased TPO mRNA levels in the TG liver; * $P < .01$. B, Increased TPO protein in the TG liver. TPO western blot analysis with α -tubulin as a loading control. The numbers below represent the relative density of TPO to α -tubulin bands. C, Increased TPO levels in TG plasma; * $P < .01$. D, Increased TPO levels in the hepatocyte conditioned medium (CM) in TG; * $P < .05$. E, Stat3 activation in the TG liver. Western blot analysis of the Stat3 phosphorylation status. The numbers below represent the relative density of phospho-Stat3 (pSTAT3) to total Stat3

from megakaryocytes.¹⁴ TPO is mainly produced by hepatocytes and interacts with the c-Mpl receptor expressed on megakaryocytic lineage cells in the bone marrow.¹⁴ qRT-PCR analysis revealed that liver TPO mRNA levels were six-fold higher in the *Alb-Cre/BRAFV600E* transgenic mice than in the normal B6 mice (Figure 3A). TPO protein levels were also increased in the liver and plasma of the *Alb-Cre/BRAFV600E* transgenic mice compared with the normal B6 mice (Figure 3B,C). Furthermore, higher levels of TPO were detected in conditioned medium collected from the cultured hepatocytes of the *Alb-Cre/BRAFV600E* transgenic mice than in medium from cultured hepatocytes from normal B6 mice (Figure 3D). TPO production by hepatocytes is upregulated by transcriptional activation of the *TPO* gene via Stat3 activation.^{15,16} Stat3 was hyperphosphorylated in the liver of the *Alb-Cre/BRAFV600E* transgenic mice compared with the normal B6 mice (Figure 3E), similar to findings for DEN-induced hepatic tumors, as previously reported.¹⁷

3.3 | Platelet deposition in hepatic sinusoids in the *Alb-Cre/BRAFV600E* transgenic mice

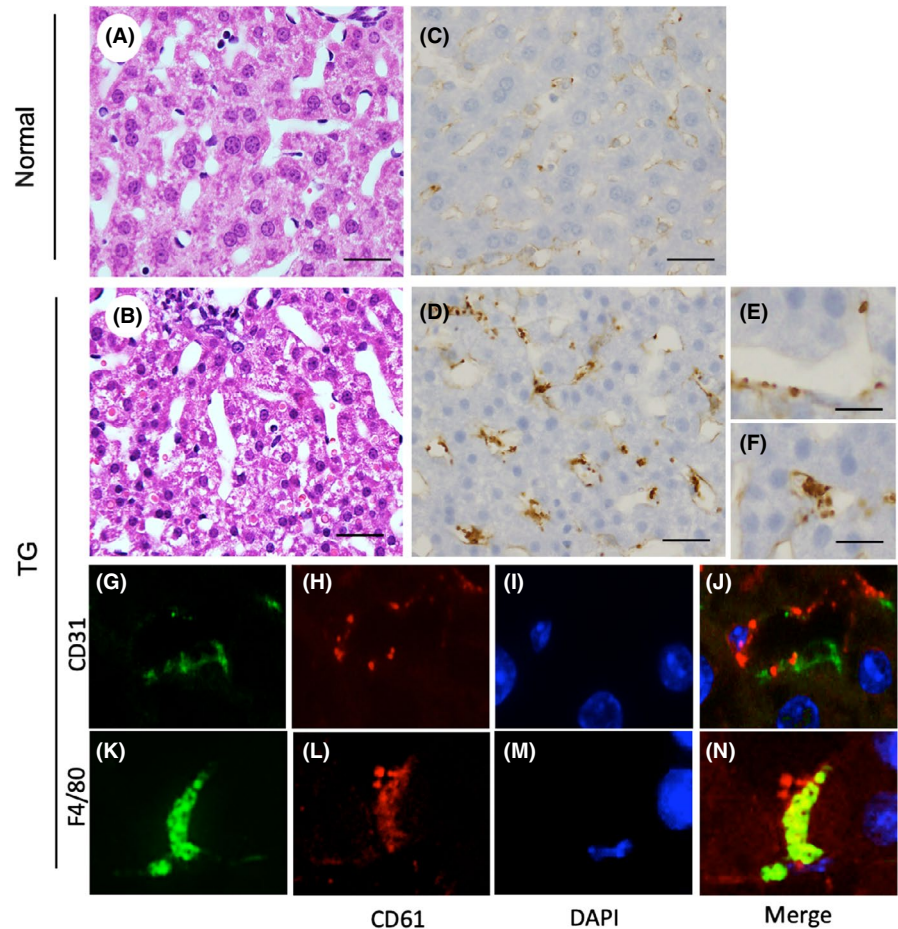
Because platelets can contribute to hepatocyte proliferation via interaction with hepatic sinusoidal cells,^{18,19} we investigated using immunohistochemistry the interaction of platelets with sinusoidal cells in the liver, which was perfused with PBS and 10% formalin in PBS to

flush out blood. Hepatocytes from *Alb-Cre/BRAFV600E* transgenic mice were characteristically basophilic and small in size, similar to DEN-induced preneoplastic hepatocytes²⁰, in contrast with those in the normal mice (Figure 4A,B). CD61 (marker of platelets) staining revealed that many platelets were deposited, either sparsely or densely, on the sinusoidal walls in the liver of *Alb-Cre/BRAFV600E* transgenic mice, in contrast with normal mice (Figure 4C,D–F). Simultaneous staining for CD61 and CD31 (the marker for sinusoidal endothelial cell [LSEC]) revealed that platelets sparsely adhered to LSECs (Figure 4G–J), while simultaneous CD61 and F4/80 (marker for Kupffer cells) staining showed that platelets densely adhered to and were incorporated into Kupffer cells (Figure 4K–N).

3.4 | Podoplanin-positive Kupffer cells in the liver of *Alb-Cre/BRAFV600E* transgenic mice

The interaction of podoplanin with CLEC-2 on platelet membranes is an important mechanism to reciprocally activate platelets and the podoplanin-expressing cells.^{9–11} Furthermore, podoplanin is expressed in activated macrophages.^{21–24} Simultaneous staining for podoplanin and F4/80 revealed that approximately 5% of F4/80-positive Kupffer cells in the liver sections of the *Alb-Cre/BRAFV600E* transgenic mice were positive for podoplanin, while no such cells were observed in the liver sections of the normal B6 mice (Figure 5A–H).

FIGURE 4 Platelet deposition in the liver sinusoids of the *Alb-Cre/BRAFV600E* transgenic mice. A, C, The liver of 8-wk-old normal B6 mice (normal), and (B, D-N) the liver of 8-wk-old *Alb-Cre/BRAFV600E* transgenic mice (TG). A, B, The TG liver consisting of small basophilic hepatocytes in contrast with the normal liver. C, D-F, Increased platelet deposition in the liver sinusoids (D), either sparse (E) or densely (F) in the TG liver in contrast to the normal liver (C). G-J, Sparse platelet deposition on the CD31-positive liver sinusoidal endothelial cells (LSEC). K-N, Dense platelet adherence/incorporation to the F4/80-positive Kupffer cells in the TG liver. A, B, H&E staining, (C-F) CD61 immunohistochemical staining, (G-J) Immunofluorescence of CD31 (green) and CD61 (red). K-N, Immunofluorescence of F4/80 (green) and CD61 (red). Scale bars: 200 μm in A-D, and 50 μm in E, F



3.5 | Other histopathological changes in the *Alb-Cre/BRAFV600E* transgenic mice

Histopathological analysis was performed on whole organs, including central nervous system (brain), respiratory (lung), digestive (alimentary tract, liver, pancreas and biliary tract), urinary (kidney and urinary bladder), endocrine (thyroid and adrenal gland), salivary (submandibular gland) and sexual organs (testis), in all of the *Alb-Cre/BRAFV600E* transgenic mice between 5 and 13 wk after birth, including those that died spontaneously. The most conspicuous changes were noted in the kidney, lung, and liver. At 5-8 wk after birth, the renal glomerular capillaries were congested with red blood cells in the *Alb-Cre/BRAFV600E* transgenic mice, in contrast with age-matched normal mice (Figure 6A,B). Immunohistochemistry for CD61 showed that many platelets were deposited in the glomeruli in the *Alb-Cre/BRAFV600E* transgenic mice, in contrast with the normal mice (Figure 6C,D). Electron microscopy revealed that platelets adhered to the glomerular endothelial cells, and podocyte foot processes were swollen and effaced in the *Alb-Cre/BRAFV600E* transgenic mice, in contrast with the normal mice (Figure 6E,F). At 13 wk after birth, cellular and extracellular matrix components were increased in Bowman's capsules, forming a crescent-shaped deposit in some of the glomeruli (Figure 6G). In lung tissue, the alveolar space was narrowed by the thickening of the alveolar septa due to congestion with red blood cells and infiltration with

mononuclear cells at 5-8 wk in the *Alb-Cre/BRAFV600E* transgenic mice, in contrast with the normal B6 mice (Figure 6H,I). CD61 staining revealed that large numbers of platelets were deposited in the alveolar septa in *Alb-Cre/BRAFV600E* transgenic mice compared with normal B6 mice (Figure 6J,K). At 13 wk after birth, the alveolar septa were thickened even more, and the alveolar space disappeared in a large area of the lungs in the *Alb-Cre/BRAFV600E* transgenic mice (Figure 6L). In addition, necrotic foci of 1-2 mm in diameter were observed in the liver of some *Alb-Cre/BRAFV600E* transgenic mice, presumably due to thrombotic embolization in the hepatic vessels (Figure 6M,N), but not in normal mice (data not shown). Although the degree of histopathological change in the kidney, lung, and liver was diverse in individual *Alb-Cre/BRAFV600E* transgenic mice, and changes tended to become more severe with age. These histopathological changes, however, were not observed in the control *BRAFV600E* mice or the normal B6 mice. There were no remarkable histological changes in other organs or tissues in the *Alb-Cre/BRAFV600E* transgenic mice (data not shown).

3.6 | Effect of Asp on the platelet activation/deposition and histopathological changes

We then investigated whether Asp, an inhibitor of platelet activation via cyclooxygenase inhibition,²⁵ can reduce platelet activation/deposition and ameliorate the histopathological changes in *Alb-Cre/*

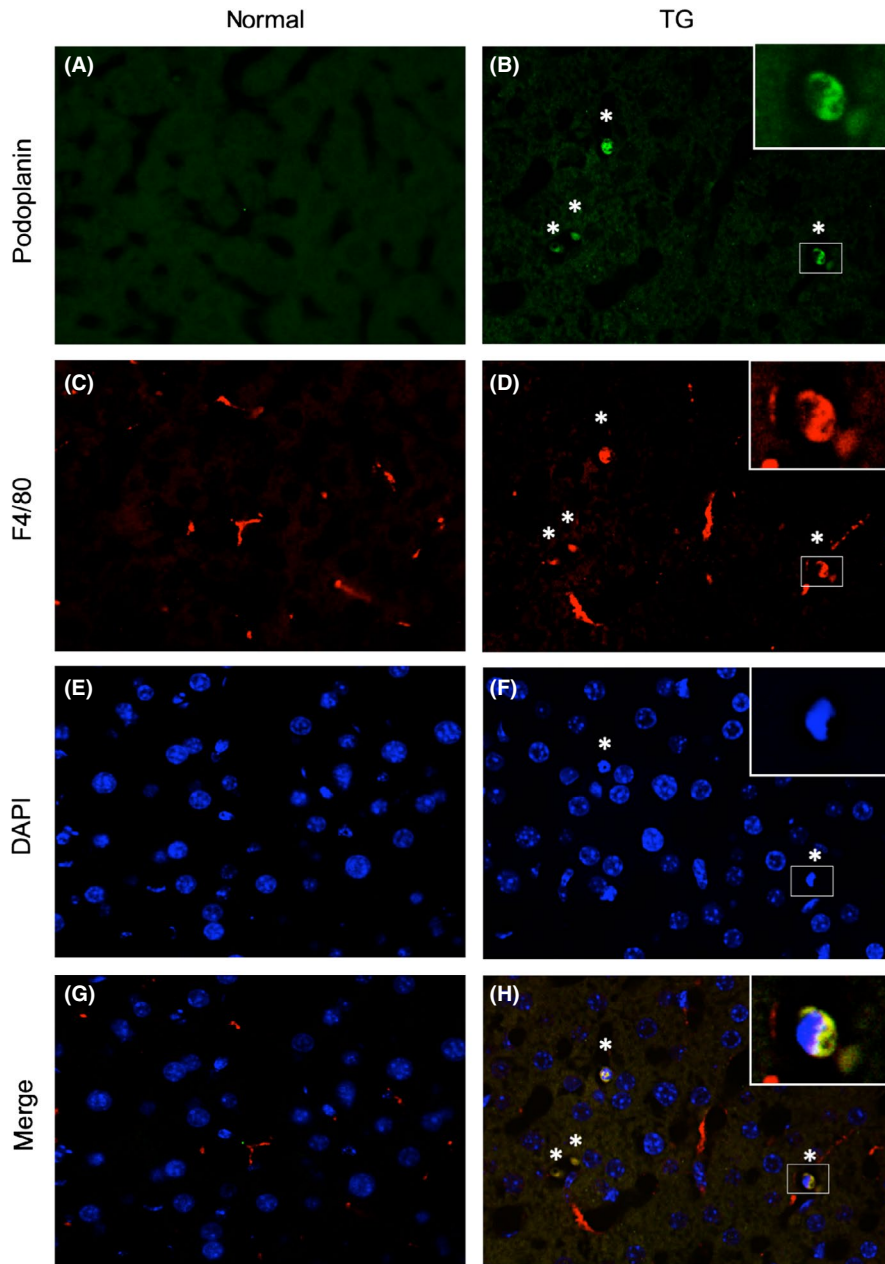


FIGURE 5 Expression of podoplanin in some of the Kupffer cells in the liver of *Alb-Cre/BRAFV600E* transgenic mice. A, C, E, G, normal; normal B6 mice and B, D, F, H, TG; *Alb-Cre/BRAFV600E* transgenic mice. A-H, Immunofluorescence of podoplanin (green) and F4/80 (red). Asterisks and insets in B, D, F, H, F4/80 and podoplanin +/+ Kupffer cells in TG liver

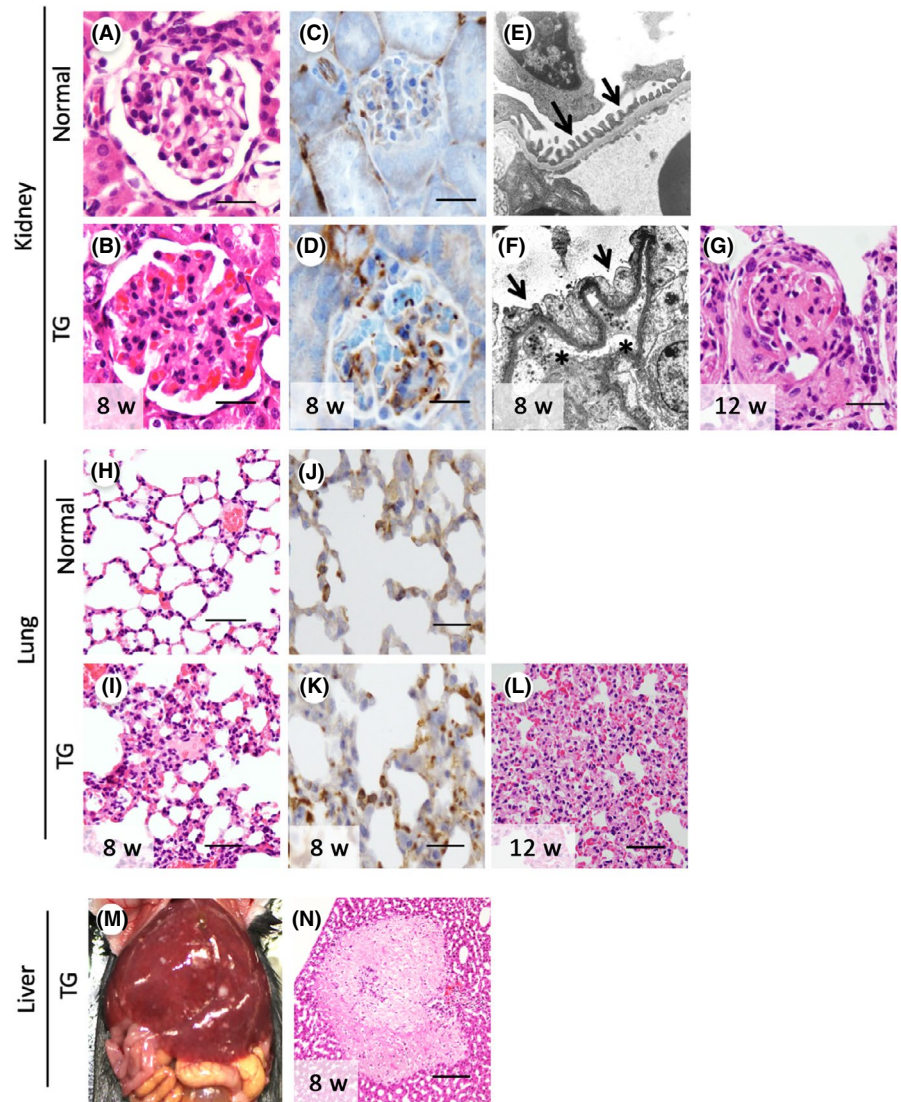
BRAFV600E transgenic mice. A daily dose of 5 $\mu\text{g/g}$ body weight Asp from 4 to 8 wk after birth decreased the PF4 levels to 35% compared with the Asp-untreated *Alb-Cre/BRAFV600E* transgenic mice (Figure 7A). Although the liver/body ratio in the Asp-untreated *Alb-Cre/BRAFV600E* transgenic mice was 4.5-fold greater than that of the control *BRAFV600E* mice, as reported previously,⁸ Asp treatment reduced the ratio to 70% in *Alb-Cre/BRAFV600E* transgenic mice, but not in the control *BRAFV600E* mice (Figure 7B). Histopathological analysis revealed that hepatocytes in the periportal areas of the hepatic lobes in the Asp-treated *Alb-Cre/BRAFV600E* transgenic mice morphologically resembled normal hepatocytes (Figure 7C-E), but such normal-looking hepatocytes were not observed in the Asp-untreated *Alb-Cre/BRAFV600E* transgenic mice. CD61 immunostaining revealed that the degree of platelet deposition was lower in the normal-looking hepatocyte areas than in the small basophilic hepatocyte

areas (Figure 7F,G). Asp administration ameliorated the renal/pulmonary changes, decreased platelet deposition in renal glomeruli and pulmonary septa (Figure 7H-K) and prevented erythrocyte dyscrasia in the *Alb-Cre/BRAFV600E* transgenic mice (Figure 7L).

3.7 | Overexpression of TPO in DEN-induced hepatic tumors and platelet deposition in sinusoids in hepatic tumors of human and mice

We lastly investigated whether TPO overproduction and platelet deposition in the sinusoids are also observed in DEN-induced hepatic tumors collected 6-12 mo after neonatal DEN treatment. As shown in Figure 8A, TPO protein levels were higher in the DEN-induced hepatic tumors compared with the surrounding normal hepatic tissues. Additionally, platelets were adhered to the

FIGURE 6 Histopathological changes in kidney, lung and liver tissues in *Alb-Cre/BRAFV600E* transgenic mice. Normal: 8-wk-old normal B6 mice and TG; 8-wk-old or 12-wk-old *Alb-Cre/BRAFV600E* transgenic mice. A-G, The kidney, (H-L) lung and (M, N) liver tissues. Opened glomerular capillary space (A), few platelet stain (C) and thin endothelial cells and podocyte processes (arrows) (E) in normal renal glomeruli. Congested capillary (B), large numbers of platelet stain (D) and swollen/effaced podocyte processes (arrows) and adherence of platelets to the capillary walls (asterisks) (F) in TG renal glomeruli 8 wk after birth. Crescent formation in Bowman's capsule in TG 12 wk after birth (G). Narrow alveolar septa (H) and few platelet stain in normal lung (J). Thickened alveolar septa (I) and increased platelet stain in the TG lung 8 wk after birth (K). Disappearance of alveolar space in the TG lung 12 wk after birth (L). Focal necrosis in the TG liver 8 wk after birth (M, N). A, B, G, H, I, L, N, H&E staining, C, D, J, K, CD61 immunohistochemistry and (E, F) electron microscopy. Scale bar: 100 μm in A, B, C, D, G, J and K, 200 μm in H, I and L, and 400 μm in N



sinusoidal cells either sparsely or densely in DEN-induced hepatic tumors (Figure 8B-E). The numbers of platelets in sinusoids were $0.37 \pm 0.08/\mu\text{m}^2$ in surrounding normal liver ($n = 3$), $1.32 \pm 0.06/\mu\text{m}^2$ in foci/adenoma ($n = 3$) and $1.23 \pm 0.35/\mu\text{m}^2$ in HCC ($n = 3$). We further investigated whether sinusoidal platelet deposition was also seen in dysplastic/neoplastic hepatic lesions in humans. CD61 immunostaining revealed that sinusoidal platelet deposition was increased in dysplastic nodules ($1.05 \pm 0.2/\mu\text{m}^2$, $n = 5$) and well differentiated HCC ($1.13 \pm 0.31/\mu\text{m}^2$, $n = 5$) compared with surrounding normal hepatic tissues ($0.25 \pm 0.06/\mu\text{m}^2$, $n = 5$) and cirrhotic nodules ($0.27 \pm 0.07/\mu\text{m}^2$, $n = 5$), but not in moderately/poorly differentiated HCC ($0.51 \pm 0.1/\mu\text{m}^2$, $n = 5$) (Figure 8F-O).

4 | DISCUSSION

In the present study, we found that mouse hepatocytes expressing the human *BRAFV600E* mutation, corresponding to the mouse *BrafV637E* mutation that is highly prevalent in DEN-induced hepatic

tumors,⁸ overproduced TPO, which led to megakaryocytosis and thrombocytosis, and that large numbers of platelets were deposited on hepatic sinusoids. TPO overproduction and sinusoidal platelet deposition were also observed in DEN-induced hepatic tumors, indicating that the observed phenomena in the *Alb-Cre/BRAFV600E* transgenic mice reflected the properties of DEN-induced hepatic tumors. Furthermore, sinusoidal platelet deposition was commonly seen in human dysplastic nodules and well differentiated HCC. This study suggested that thrombocytosis, platelet activation, and interaction of platelets to sinusoidal cells promotes hepatocarcinogenesis from an early stage via TPO overproduction by preneoplastic/neoplastic hepatocytes. These results are consistent with previous reports that HCC patients occasionally present thrombocytosis, which is correlated with an unfavorable prognosis, when TPO is overproduced by HCC cells.²⁶⁻²⁸

Thrombopoietin production by hepatocytes is enhanced by transcriptional activation of the TPO gene via the Stat3 pathway.^{15,16} In our present study, we found that Stat3 was hyperphosphorylated, as observed in the DEN-induced hepatic tumors.¹⁷ Although the exact

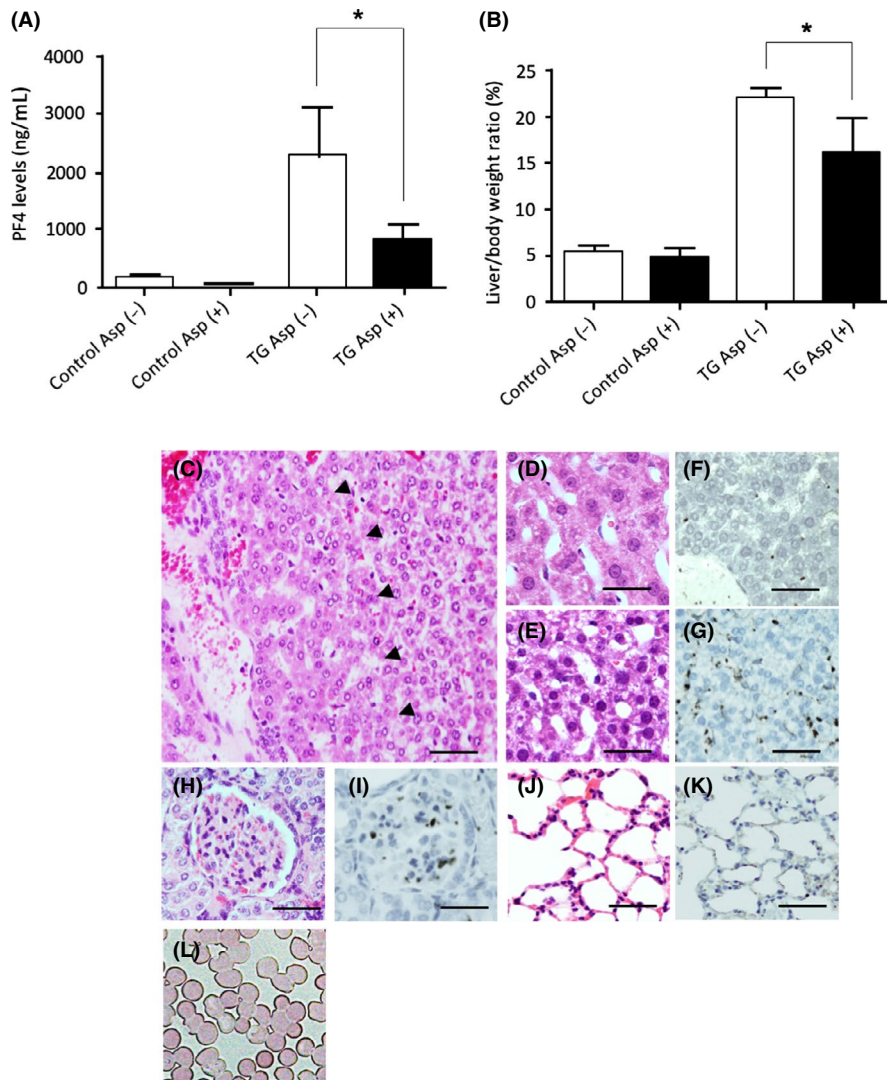


FIGURE 7 Effect of Asp on platelet activation/deposition and pathological changes in the *Alb-Cre/BRAFV600E* transgenic mice. A, B, control; control *BRAFV600E* mice and TG; *Alb-Cre/BRAFV600E* transgenic mice. A, Decreased platelet factor 4 (PF4) levels in Asp-treated TG in comparison with Asp-untreated TG. * $P < .05$. B, Decreased liver/body weight ratio in Asp-treated TG in comparison with Asp-untreated TG. * $P < .05$. C-E, Normal-looking hepatocytes (C arrowheads and D) together with small basophilic hepatocytes (E) in the liver of Asp-treated TG. F, G, Reduced platelet deposition in the normal-looking hepatocyte area (F) compared with the small basophilic hepatocyte area (G) in the liver of Asp-treated TG. H-K, Amelioration of the renal glomerular (H) and pulmonary interstitial changes (J) associated with reduced platelet deposition (I, K) in Asp-treated TG. C-E, H, J: H&E staining. F, G, I, K: CD61 immunostaining. Scale bars: 200 μm in C, F-K and 100 μm in D, E, L. No erythrocyte dyscrasia in Asp-treated TG

reason(s) for Stat3 activation is not known at present, it is possible that factors derived from activated platelets and/or sinusoidal cells might activate Stat3 in hepatocytes. It is also possible that, because DEN-induced hepatic tumor cells in which the *Braf* mutation is highly prevalent express various growth factors, cytokines, chemokines and their receptors,^{8,29-33} these autocrine factors and their receptors may contribute to Stat3 activation.

Platelets adhered sparsely to LSECs and densely adhered to and were incorporated into Kupffer cells in the livers of *Alb-Cre/BRAFV600E* transgenic mice, which has also been reported in the regenerating liver.^{18,19} Because the liver was perfused with PBS and formalin solution to flush out blood cells, platelets were tightly adhered to the sinusoidal cells in the liver of *Alb-Cre/BRAFV600E* transgenic mice. Compelling evidence indicates that platelets play an important role in liver homeostasis and pathobiology by interacting with hepatic cells, including LSECs, Kupffer cells, hepatic stellate cells, and hepatocytes, and by releasing bioactive substances.^{18,19} The factors derived from both platelets and platelet-activated sinusoidal cells can stimulate various intracellular signaling pathways in hepatocytes, including the NF- κ B, Stat3, MAPK/ERK and PI3K/

Akt pathways.^{18,19} The sinusoidal platelet deposition indicated that platelets contribute to hepatocyte proliferation in the *Alb-Cre/BRAFV600E* transgenic mice as well as in hepatic tumor cells.

In the *Alb-Cre/BRAFV600E* transgenic mice, platelets were thought to be activated in the peripheral blood because plasma PF4 levels were elevated and because some of the platelets were increased in size, which is the characteristic feature of activated platelets.³⁴ Conversely, schizocytes were observed in the peripheral blood smear samples, indicating that erythrocytes were damaged. Aberrant platelet activation causes thrombotic microangiopathy, which leads to erythrocyte dyscrasia.¹² However, the platelet numbers are usually decreased in thrombotic microangiopathy,¹² and the TPO levels are commonly decreased in association with thrombocytosis because TPO is bound to the platelet c-Mpl receptor, internalized, and destroyed.³⁵ In the *Alb-Cre/BRAFV600E* transgenic mice, however, continuous TPO overproduction by *BRAFV600E*-mutated hepatocytes might maintain the high circulating TPO levels and increase the number of platelets.

In the liver of *Alb-Cre/BRAFV600E* transgenic mice, some Kupffer cells were positive for podoplanin. In these physiological conditions,

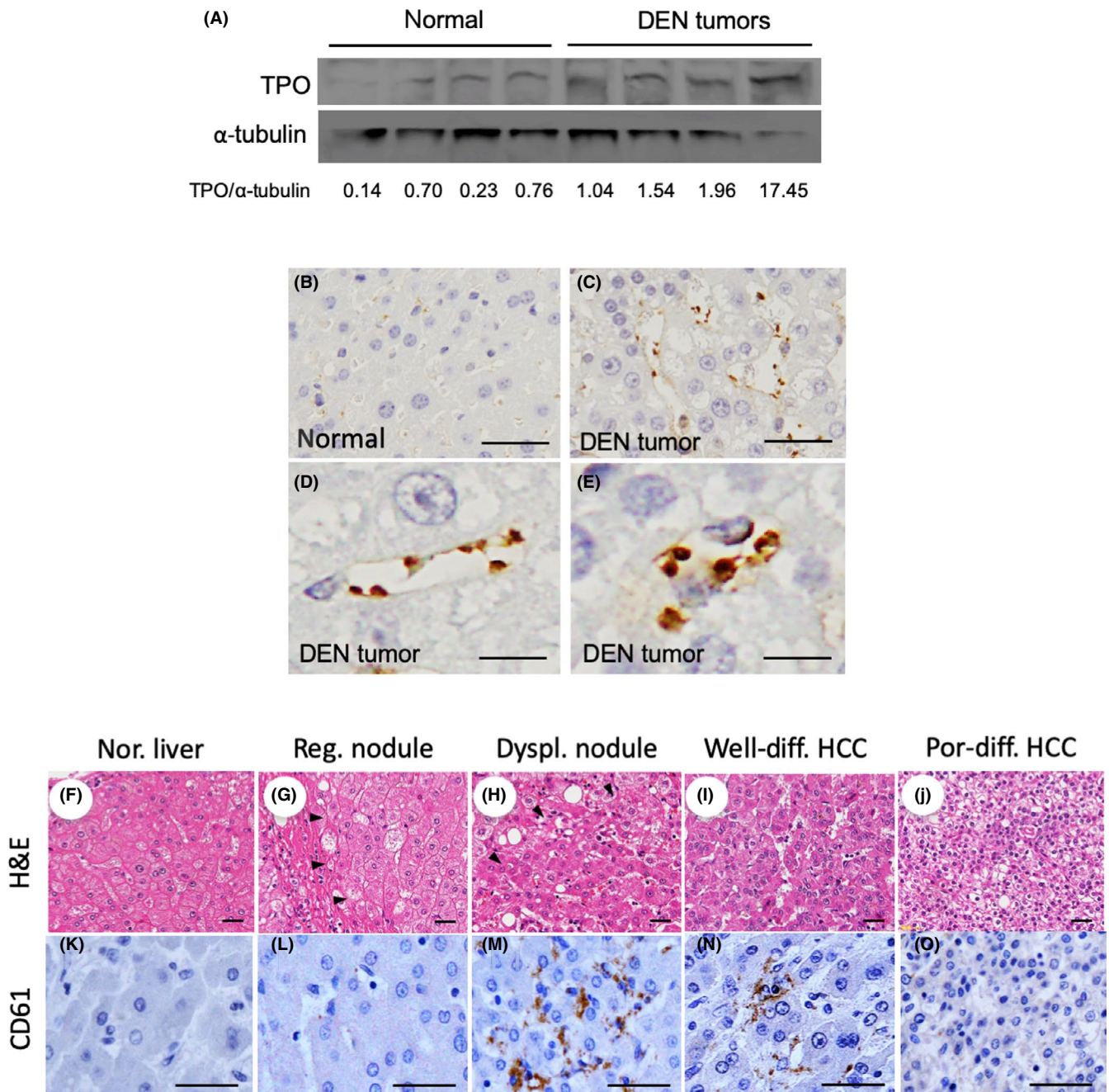


FIGURE 8 Thrombopoietin (TPO) overproduction in diethylnitrosamine (DEN)-induced hepatic tumors and platelet deposition in sinusoids in hepatic tumors in human and mice. A, Western blot analysis of TPO in the normal hepatic tissue (normal) and DEN-induced hepatic tumors collected 8–12 mo of age (DEN tumors). The numbers below represent the relative density of TPO to α -tubulin bands. Increased numbers of platelets deposited in the sinusoids of DEN tumors (C), either sparsely (D) or densely (E). Increased platelet deposition in sinusoids in the human dysplastic nodules (H, M) and well differentiated HCC (I, N) compared with normal liver (F, K) and regenerating cirrhotic nodules (G, L), but not in poorly differentiated HCC (J, O). B–E, K–O: Immunohistochemical staining of CD61. F–J, H&E staining. Scale bars: 100 μ m in B, C, F–O and 25 μ m in D, E

although podoplanin is expressed in some kinds of cells such as kidney podocytes, lung alveolar type I cells and lymphatic endothelial cells, these cells do not directly interact with platelets.^{9–11} In the *Cre-Alb/BRAFV600E* transgenic mice, however, podoplanin-positive Kupffer cells might trigger aberrant platelet activation via the interaction of podoplanin with platelet CLEC-2, which facilitates platelets to interact with Kupffer cells and LSECs in the liver and to be

deposited in the renal glomeruli and the pulmonary alveoli. Platelet activation through the interaction of CLEC-2 with podoplanin expressed in sinusoidal cells was also shown in regenerating liver tissue after a two-thirds hepatectomy in mice.³⁶ There are two subsets of hepatic macrophages: yolk sac/fetal liver-derived and bone marrow/monocyte-derived macrophages.^{37–39} Conversely, although podoplanin is generally not expressed in macrophages, it is expressed in

activated macrophages such as those treated with thioglycollate or lipopolysaccharide in vitro,²¹ in those found in the liver of *Salmonella*-infected mice,²² in those found in the spleen and peritoneal cavity in zymosan-treated mice²³ and in severe atherosclerotic lesions in humans.²⁴ It is thought that, in the hepatic microenvironment of *Alb-Cre/BRAFV600E* transgenic mice, a subset of resident macrophages or those recruited from outside of the liver might be influenced to express podoplanin.

In the *Alb-Cre/BRAFV600E* transgenic mice, platelets were deposited in the kidney and lung, as well as in the liver. Because platelet-derived factors promote the recruitment/activation of inflammatory cells and the migration/proliferation of mesenchymal cells,⁴⁰ platelet deposition in renal glomeruli and pulmonary alveoli may be related to the pathogenesis of glomerulonephropathy and interstitial pneumonia in *Alb-Cre/BRAFV600E* transgenic mice. Interestingly, the tissues where platelets were deposited contained podoplanin-expressing cells: podocytes in the renal glomeruli and type 1 alveolar cells in the lung.⁹⁻¹¹ Thus, tissue destruction due to the deposition of activated platelets might have enabled an interaction between platelet CLEC-2 and podoplanin-expressing cells, further aggravating inflammation and tissue destruction. However, it remains to be investigated whether platelets directly interact with podoplanin-expressing cells in the kidney and lung.

In the *Alb-Cre/BRAFV600E* transgenic mice, Asp, a platelet activation inhibitor via cyclooxygenase inhibition,²⁵ efficiently prevented platelet activation and ameliorated the histopathological changes in association with decreased platelet deposition in the liver, kidney, and lung. These observations indicate that the pathological changes in these organs are dependent on the deposition of aberrantly activated platelets. Interestingly, the liver/body weight ratio was decreased to 70% in the Asp-treated *Alb-Cre/BRAFV600E* transgenic mice, and normal-looking hepatocyte areas were specifically observed together with small basophilic hepatocytes. Furthermore, the degree of sinusoidal platelet deposition was lower in the normal-looking hepatocyte areas than in the small basophilic hepatocyte areas. These observations suggested that the properties of *BRAFV600E*-mutated hepatocytes were regulated by sinusoidal platelet deposition.

In conclusion, the macroenvironment that results from TPO overproduction by the preneoplastic/neoplastic hepatocytes, eventual megakaryocytosis/thrombocytosis, and platelet activation and interaction with hepatic sinusoidal cells may contribute to hepatocarcinogenesis from a very early stage. However, erythrocyte dyscrasia, presumably due to thrombotic microangiopathy, and glomerulonephropathy/interstitial pneumonia due to platelet deposition caused spontaneous death.

ACKNOWLEDGMENTS

This study was supported by Grant-in-Aid for the Japanese Ministry of Education, Culture, Sports, Science and Technology (JSPS KAKENHI grant no. JP16K14615) to KY. We thank the staff of the New Drug Research Center, Eniwa, Hokkaido, Japan for technical

assistance and animal care. The authors would like to thank Seiji Ohtani for his technical assistance in our experiments.

DISCLOSURE

No conflict of interest.

ORCID

Katsuhiko Ogawa  <https://orcid.org/0000-0002-0319-0765>

REFERENCES

- Sia D, Villanueva A, Friedman SK, Llovet JM. Liver cancer cell of origin, molecular class, and effects on patient prognosis. *Gastroenterology*. 2017;152:745-761.
- Heindryckx F, Colle I, Van Vlierberghe H. Experimental mouse models for hepatocellular carcinoma research. *Int J Exp Pathol*. 2009;90:367-386.
- Goldfarb S, Pugh TD, Koen H, He YZ. Preneoplastic and neoplastic progression during hepatocarcinogenesis in mice injected with diethylnitrosamine in infancy. *Environ Health Perspect*. 1983;50:149-161.
- Buchmann A, Bauer-Hofmann R, Mahr J, Drinkwater NR, Luz A, Schwarz M. Mutational activation of the c-Ha-ras gene in liver tumors of different rodent strains: correlation with susceptibility to hepatocarcinogenesis. *Proc Natl Acad Sci USA*. 1991;88:911-915.
- Dragani TA, Manenti G, Colombo BM, et al. Incidence of mutation at codon 61 of the Ha-ras gene in liver tumors of mice genetically susceptible and resistant to hepatocarcinogenesis. *Oncogene*. 1991;6:333-338.
- Jaworski M, Buchmann A, Bauer P, Riess O, Schwarz M. B-Raf and Ha-ras mutations in chemically induced mouse liver tumors. *Oncogene*. 2005;24:1290-1295.
- Buchmann A, Karcier Z, Schmid B, Strathmann J, Schwarz M. Differential selection for B-raf and Ha-ras mutated liver tumors in mice with high and low susceptibility to hepatocarcinogenesis. *Mutat Res*. 2008;638:66-74.
- Yamamoto M, Tanaka H, Xin B, et al. Role of the BrafV637E mutation in hepatocarcinogenesis induced by treatment with diethylnitrosamine in neonatal B6C3F1 mice. *Mol Carcinog*. 2017;56:478-488.
- Navarro-Nunez L, Langan SA, Nash GB, Watson SP. The physiological and pathophysiological roles of platelet CLEC-2. *Thromb Haemost*. 2013;109:991-998.
- Suzuki-Inoue K, Osada M, Ozaki Y. Physiologic and pathophysiologic roles of interaction between C-type lectin-like receptor 2 and podoplanin: partners from in utero to adulthood. *J Thromb Haemost*. 2017;15:219-229.
- Renert L, Carrasco-Ramirez P, Fernandez-Munoz B, et al. New insights into the role of podoplanin in epithelial-mesenchymal transition. *Int Rev Cell Mol Biol*. 2015;317:185-239.
- Shatzel JJ, Taylor JA. Syndromes of thrombotic microangiopathy. *Med Clin North Am*. 2017;101:395-415.
- Kaplan KL, Owen J. Plasma levels of β -thromboglobulin and platelet factor 4 as indices of platelet activation in vivo. *Blood*. 1981;57:199-202.
- Akkerman JW. Thrombopoietin and platelet function. *Semin Thromb Hemost*. 2006;32:295-304.
- Kaser A, Brandacher G, Steurer W, et al. Interleukin-6 stimulates thrombopoiesis through thrombopoietin: role in inflammatory thrombocytosis. *Blood*. 2001;98:2720-2725.
- Burmester H, Wolber EM, Freitag P, Fandrey J, Jelkmann W. Thrombopoietin production in wild-type and interleukin-6

- knockout mice with acute inflammation. *J Interferon Cytokine Res.* 2005;25:407-413.
17. Miyakoshi M, Yamamoto M, Tanaka H, Ogawa K. Serine 727 phosphorylation of STAT3: an early change in mouse hepatocarcinogenesis induced by neonatal treatment with diethylnitrosamine. *Mol Carcinog.* 2014;53:67-76.
 18. Meyer J, Lejmi E, Fontana P, Morel P, Gonelle-Gispert C, Bühler L. A focus on the role of platelets in liver regeneration: do platelet-endothelial cell interactions initiate the regenerative process? *J Hepatol.* 2015;63:1263-1271.
 19. Chauhan A, Adams DH, Watson SP, Lalor PF. Platelets: no longer bystanders in liver disease. *Hepatology.* 2016;64:1774-1784.
 20. Thoolen B, Maronpot RR, Harada T, et al. Proliferative and nonproliferative lesions of the rat and mouse hepatobiliary system. *Toxicol Pathol.* 2010;38:55-81S.
 21. Kerrigan AM, Navarro-Nunez L, Pyz E, et al. Podoplanin-expressing inflammatory macrophages activate murine platelets via CLEC-2. *J Thromb Haemost.* 2012;10:484-486.
 22. Hitchcock JR, Cook CN, Bobat S, et al. Inflammation drives thrombosis after Salmonella infection via CLEC-2 on platelets. *J Clin Invest.* 2015;125:4429-4445.
 23. Hou TZ, Bystrom J, Sherlock JP, et al. A distinct subset of podoplanin (gp38) expressing F4/80+ macrophages mediate phagocytosis and are induced following zymosan peritonitis. *FEBS Lett.* 2010;584:3955-3961.
 24. Hatakeyama K, Kaneko MK, Kato Y, et al. Podoplanin expression in advanced atherosclerotic lesions of human aortas. *Thromb Res.* 2012;129:e70-e76.
 25. Catella-Lawson F, Reilly M, Kapoor SK, et al. Cyclooxygenase inhibitors and the antiplatelet effects of aspirin. *N Engl J Med.* 2001;345:1809-1817.
 26. Carr BI, Guerra V. Thrombocytosis and hepatocellular carcinoma. *Dig Dis Sci.* 2013;58:1790-1796.
 27. Hwang SJ, Luo JC, Li CP, et al. Thrombocytosis: a paraneoplastic syndrome in patients with hepatocellular carcinoma. *World J Gastroenterol.* 2004;10:2472-2477.
 28. Bihari C, Rastogi A, Shasthry SM, et al. Platelets contribute to growth and metastasis in hepatocellular carcinoma. *APMIS.* 2016;124:776-786.
 29. Ishizaki T, Yoshie M, Yaginuma Y, Tanaka T, Ogawa K. Loss of Igf2 imprinting in monoclonal mouse hepatic tumor cells is not associated with abnormal methylation patterns for the H19, Igf2, and Kvlqt1 differentially methylated regions. *J Biol Chem.* 2003;278:6222-6228.
 30. Tanno S, Ogawa K. Abundant TGF α precursor and EGF receptor expression as a possible mechanism for the preferential growth of carcinogen-induced preneoplastic and neoplastic hepatocytes in rats. *Carcinogenesis.* 1994;15:1689-1694.
 31. Kishibe K, Yamada Y, Ogawa K. Production of nerve growth factor by mouse hepatocellular carcinoma cells and expression of TrkA in tumor-associated arteries in mice. *Gastroenterology.* 2002;122:1978-1986.
 32. Tanaka H, Yamamoto M, Hashimoto N, et al. Hypoxia-independent overexpression of hypoxia-inducible factor 1 α as an early change in mouse hepatocarcinogenesis. *Cancer Res.* 2006;66:11263-11270.
 33. He G, Dhar D, Nakagawa H, et al. Identification of liver cancer progenitors whose malignant progression depends on autocrine IL-6 signaling. *Cell.* 2013;155:384-396.
 34. Gremmel T, Frelinger AL III, Michelson AD. Platelet physiology. *Semin Thromb Hemost.* 2016;42:191-204.
 35. Fielder PJ, Gurney AL, Stefanich E, et al. Regulation of thrombopoietin levels by c-mpl-mediated binding to platelets. *Blood.* 1996;87:2154-2161.
 36. Kono H, Fujii H, Suzuki-Inoue K, et al. The platelet-activating receptor C-type lectin receptor-2 plays an essential role in liver regeneration after partial hepatectomy in mice. *J Thromb Haemost.* 2017;15:1-11.
 37. Naito M, Hasegawa G, Takahashi K. Development, differentiation, and maturation of Kupffer cells. *Micro Res Tech.* 1997;39:350-364.
 38. Klein I, Cornejo JC, Polakos NK, et al. Kupffer cell heterogeneity: functional properties of bone marrow-derived and sessile hepatic macrophages. *Blood.* 2007;110:4077-4085.
 39. Ikarashi M, Nakashima H, Kinoshita M, et al. Distinct development and functions of resident and recruited liver Kupffer cells/macrophages. *J Leukoc Biol.* 2013;94:1325-1336.
 40. Nurden AT. Platelets, inflammation and tissue regeneration. *Thromb Haemost.* 2011;105:S13-S33.

How to cite this article: Tanaka H, Horioka K, Yamamoto M, et al. Overproduction of thrombopoietin by BRAFV600E-mutated mouse hepatocytes and contribution of thrombopoietin to hepatocarcinogenesis. *Cancer Sci.* 2019;110:2748-2759. <https://doi.org/10.1111/cas.14130>